LOW-ORDER MODELLING AND VALIDATION OF FILM COOLING IN LIQUID ROCKET COMBUSTION CHAMBERS

Pierluigi Concio [(1)], Simone D'Alessandro [(2)], Maria Aranda-Rosales[(3)], Daniele Bianchi[(4)], Francesco Nasuti [(5)], Johan Steelant[(6)]

[(1)] Sapienza University of Rome, Via Eudossiana 18, 00184 Italy, Email: pierluigi.concio@uniroma1.it
[(2)] Sapienza University of Rome, Via Eudossiana 18, 00184 Italy, Email: simone.dalessandro@uniroma1.it
[(3)] Empresarios Agrupados Internacional, Madrid, Spain, Email: maranda@empre.es
[(4)] Sapienza University of Rome, Via Eudossiana 18, 00184 Italy, Email: daniele.bianchi@uniroma1.it
[(5)] Sapienza University of Rome, Via Eudossiana 18, 00184 Italy, Email: francesco.nasuti@uniroma1.it
[(6)] ESTEC-ESA, Noordwijk, Netherlands, Email: johan.steelant@esa.int

KEYWORDS: film cooling, thrust chamber, liquid rocket engine

ABSTRACT:

Active chamber cooling systems are often required in liquid rocket engines design to suitably extract heat from the hot-gas flow and maintain a reasonably low wall temperature. In the design process, numerical simulations are often necessary to reduce the number of expensive hot-firing tests. In this sense, the European Space Propulsion System Simulation (ESPSS) framework has been developed to simulate complex systems steady-state and transient analyses. The inclusion of film cooling low-order modeling represents a useful tool during the engine development phase allowing quick evaluations of such a complex phenomenon in a system-wide representation, where interdependence with other phenomena might occur.
The implemented formulation aims to predict the main features of a film-cooled liquid rocket combustion chamber. Reliability of such predictions is assessed by comparing the steady-state results with experimental test cases and CFD simulations.
Comparisons show that the errors on the prediction of the different engine features spans between 2 and 20%, depending on the specific quantity observed and on the specific test case.

1. INTRODUCTION

Film cooling is a cooling method used in liquid rocket engines (LRE) to protect combustion chamber and nozzle walls against high thermal loads. A controlled flow of coolant is introduced either in liquid or gaseous phase as a thin film through slots or discrete holes, placed in the combustion chamber, for example at the outer row of the faceplate or at different positions downstream, or in specific nozzle planes toward the throat. The amount of mass flow rate that is typically used for this purpose is in the range between 1 and 6% of the total mass flow rate, yielding of course some performance loss. Film cooling might represent an interesting choice, especially when in combination with other cooling techniques such as regenerative cooling, achieving high performances and protecting those engines which operate at significantly high pressure, and thus undergo significantly high thermal loads.

The EcosimPro/ESPSS platform [28] allows such a propulsion system to be assembled and simulated by connecting the individual components available in the software, and furthermore it allows to design and develop brand-new components to be included in the model in turn.
Low-order LRE thrust chamber film cooling models have been searched in the literature and selected accordingly to the EcosimPro/ESPSS framework paradigm and capabilities.
This paper aims at presenting a new component based on a liquid and gaseous film-cooled thrust chamber to be included in the ESPSS simulation platform, hence enriching and improving its heat loads prediction capabilities.
The new formulation is assessed by analyzing transients flow evolution and comparing the steady-state results with the selected experimental test cases and purposely carried out CFD simulations performed using an in-house RANS-based CFD solver.

2. STATE OF THE ART

The main results concerning liquid and gaseous film cooling modeling developed since the '50s and available in the literature have been reviewed. Particular attention has been paid to numerical and modeling aspects in liquid rocket engines combustion chambers and nozzles.
Three peculiar and particularly challenging aspects can be defined for Liquid Film Cooling (LFC), i.e the liquid film stability, its phase change (evaporation), and the extension of the wall wet by the film and identified by the Film Cooled Length (FCL). In particular, the FCL is defined as the length after which the film ceases to exist in liquid

phase, thus changing completely the cooling performance.
The determination of the evaporation rate for both inert and reactive coolants was the subject of the early analytical and empirical studies [1, 2], retaining a lot of assumptions to obtain results in closed form, and hence yielding very limited applicability in some cases [3, 4]. Unrealistic treatments of film stability also led to high discrepancies in later numerical studies [5]. Different attempts have been made to develop correlations accounting also for the entrainment of liquid droplets in the gaseous phase [6, 7]. Even nowadays, the liquid entrainment and film stability phenomena are not understood enough to give definitive conclusions [8], and no experimental information is available for assessment under rocket engine-like conditions. From the modeling point of view, the correlation by Sawant et al. [7] represents a reasonable choice.
Semi-analytical, 1-D differential and 0-D algebraic formulations have been developed including also liquid entrainment and hot gas radiation modeling for the calculation of FCL and the evaporation rate [9, 11, 12]. Overall overestimations were shown by the former, with a fair matching with experimental data [10], whereas good agreements are provided by the latter two. Those models introduce some heavy computations, such as the implicit calculation of several quantities, so lighter explicit models [9, 11] have been proposed yielding a compromise between accuracy and computational cost.

Concerning Gaseous Film Cooling (GFC) investigations, they were dedicated to understand the effects of different coolant injection procedures [13], free stream turbulence level [14], and compressibility [15] on the main stream boundary layer. It was found that multi-slot injection is more suited for high energy propellants, for example hydrogen and methane, and that no significant changes of cooling performance occur because of variations in the turbulence intensity of the coolant jet. Gas compressibility is found to change the growth rate of the shear layer between the main and secondary flow.
The determination of GFC performance has been mostly carried out empirically. A great number of studies and results is available in open literature concerning gaseous film cooling, but, unfortunately, only few recent numerical analyses have been carried out aiming to study of rocket thrust chambers. Some correlations have been proposed [16], typically in terms of film cooling effectiveness. Those models assume constant properties ideal gases, a constant average temperature in the boundary layer, and a full mixing of the coolant with the core flow. Significant improvements have been made [17-20], proposing further dependencies and modelling of phenomena occurring in rocket combustion chambers.

3. IMPLEMENTATION

In the new component, the implemented formulation aims at predicting the main features of a film-cooled combustion chamber, namely, i) the film extension before complete mixing/entrainment occurs (in case of gaseous/liquid coolant, respectively), ii) the effective reduction of wall heat flux in the cooled region, iii) the O/F ratio shift resulting from film addition and its effect on performance, while retaining reasonable computational times due to its inclusion in the ESPSS multi-physics platform.

The film-cooled thrust chamber component has been implemented as two new components (see *Figure **1**. New film-cooled thrust chamber super-components: LFC (left) and GFC (right)*), making a distinction between liquid and gaseous film cooling. The motivation lies in the fact that it needed invasive and different modifications, with respect to the regular liquid combustor, due to the complex nature of the problem. In fact, the presence of the coolant affects both the heat flux to the walls and the hot gas flow behaviour inside the chamber, influenced by coolant vaporization and reaction. The original nozzle component has been employed retaining the same super-component overall topology.

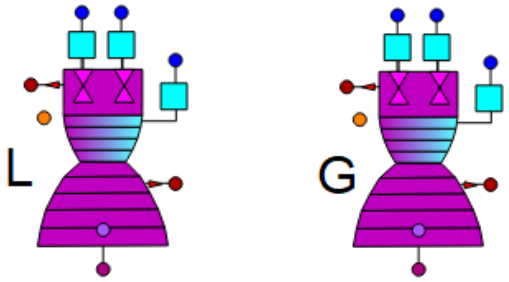

Figure 1. New film-cooled thrust chamber super-components: LFC (left) and GFC (right)

Concerning liquid film cooling, the model uses the hot-gas flow thermodynamic state and properties as inputs (in compliance with the model requirements) to compute a fixed set of quantities, i.e., evaporation rate, heat fluxes, boundary layer mass flow rate and temperature, which are calculated at each time step, according to the chosen model features. Film injection can take place at any chamber node, retaining the regular combustor solution prior to injection. No restrictions apply concerning the coolant species choice, as it can be chosen as one of the propellants or a third different fluid. Mixtures are also allowed by the component.

The hot gases and the coolant are considered as two separate entities, until evaporation occurs. Such dynamics has been included in all the flow

conservation laws as a distributed mass flow rate source term along the chamber, and thus correctly generates different phenomena, as follows (note that such dynamics occurs between the liquid film and the hot flow).

i. Chamber pressure increases due to the injected additional mass flow rate.

ii. Enthalpy content of the inflowing flux influences chamber temperature.

iii. Coolant chemicals react with the hot gases, influencing the hot mixture composition (O/F shift) and thus its temperature.

iv. Heat loss term in the energy equation also includes the heat transferred from the hot gas to the film.

It has to be remarked that the coolant evaporation process and the thermochemical state of the hot gas stream in its vicinity are interdependent. For such a reason, an iterative procedure is necessary to compute the correct coupling between heat load to the film and the hot stream state in its vicinity.

Concerning gaseous film cooling the logic is similar, except for the evaporation process, which is not present of course. Hot gases, film, and mixing regions are treated independently in the combustor, and then assembled together depending on the computed flowfield geometry to eventually provide the wall heat flux distribution.

4. NUMERICAL MODELS

Because of the nature of the ESPSS framework, different categories of models which can deliver results with different orders of accuracy with respect to the investigated phenomena have been selected in the literature, thus involving different computational efforts; concerning both gaseous and liquid film cooling. On the basis of the performed literature review, models considered as the best candidates for the implementation are presented in the following. In particular, the first three models are for LFC while the last one concerns GFC.

4.1. Grisson

Grisson model [11] is a one-dimensional analytical model of liquid film cooling in liquid rocket engine combustion chambers. The main purpose of the model is to calculate the coolant evaporation rate due to heating and, as a consequence, to estimate the size of the film cooled region, i.e., the length after which the film ceases to exist in liquid phase. Radiative heating is considered in such phase. Grisson's complete model also assumes that a portion of the evaporated coolant continues to provide a (lesser) thermal protection due to its entrainment into the boundary layer. Limitations exist for this model, e.g., since liquid drops entrainment into the hot gas stream is neglected, applying the model to small coolant mass flow rates is recommended. Moreover, the effect of boundary-layer gases acceleration is neglected as well, so lower accuracy is expected in the nozzle (a correction factor exists only for the convergent section).
Right after injection, the coolant is assumed to heat up until saturation conditions due to heat exchange with the hot gases. The convective heat transfer coefficient is calculated with the hot gas properties according to the flat plate correlation by Chilton and Colburn. The convective heat exchange between the film and the walls is evaluated using the same procedure while considering the liquid coolant properties. The radiative heat flux towards the liquid film and towards the chamber wall is also evaluated. Hot-gas total emittance is evaluated through the model. The total heat flux is absorbed by the liquid film, causing a temperature rise and, after the liquid reaches the saturation temperature, the evaporation rate per unit area is calculated iteratively by the following system of algebraic equations:

$$\dot{m}_{vap} = \frac{Q_{conv,film} + Q_{rad,film} + Q_{conv,film}^{WALL}}{\lambda} \qquad \text{Eq.1}$$

$$\frac{h}{h_0} = \frac{\ln(1+H)}{H} \qquad \text{Eq.2}$$

$$H = \frac{K_m c_{p,g}}{\lambda}\left[\left(T_g - T_{sat}\right) + \frac{Q_{rad,film}}{h}\right] = \frac{K_m c_{p,g}\dot{m}_{vap}}{h} \qquad \text{Eq.3}$$

where: $\dot{m}_{vap}$ is the evaporation rate, $Q_{conv,film}$ and $Q_{rad,film}$ are the convective ad radiative heat fluxes entering the liquid film, λ is the latent heat of vaporization, h_0 is the convective heat transfer coefficient, h is the transpiration-corrected convective heat transfer coefficient, $c_{p,g}$ is the hot gas specific heat at constant pressure, K_m is a correction factor depending on hot gas and film molar masses, T_g is the hot gas temperature, and T_{sat} is the liquid film saturation temperature.

The vapor flows away from the liquid film, similar to liquid transpiration through a porous wall, thus decreasing the wall shear stress and convective heat flux. To take into account this phenomenon, a new convective heat transfer coefficient and a new

wall shear stress are calculated from the old ones (h_0, τ_0) by means of the transpiration correction h/h_0.

Once the evaporation rate is known, it decreases the liquid mass flow rate per unit circumference at a rate $\frac{\Delta\Gamma}{\Delta x} = -\dot{m}_{vap}$. The film cooled length FCL is hence determined as the abscissa at which $\Gamma = 0$. Starting from the position marked as FCL it is assumed that the whole coolant mass remains in the boundary layer, and it heats up due to the free stream entrainment. Once the boundary layer temperature is obtained, the convective heat transfer coefficient between the boundary layer and the walls is calculated according to the Chilton-Colburn correlation as above.

4.2. Grisson (simplified)

Grisson [11] also provided a simplified 0-D analytical formulation of his model to avoid the iterative calculation of the evaporation rate and the transpiration-corrected convective heat transfer coefficient. It can be obtained explicitly by neglecting radiation toward the liquid film. In such a way, the transpiration correction reduces to a simple form, and the FCL can be calculated according to the following equation without the necessity of integrating along the chamber abscissa:

$$FCL = \frac{61.62\mu_g}{G_{mean}}\left[\frac{\lambda^*\Gamma\, Pr^{0.94}}{c_{p,g}(T_g - T_{sat})\mu_g\left(\frac{h}{h_0}\right)}\right]^{1.25} \qquad \text{Eq.4}$$

where: μ_g is the hot gas dynamic viscosity, G_{mean} is a modified hot gas mass flux (see [11] for details), $\lambda^* = \lambda + c_{p,liq}(T_{sat} - T_{liq})$, Γ is the liquid film mass flow rate per unit chamber circumference, $c_{p,liq}$ is the liquid film specific heat at constant pressure and T_{liq} is the film injection temperature.

4.3. Shine et al.

Shine et al. model [12] is a 0-dimensional analytical model of film cooling in liquid rocket engine combustion chambers operating at subcritical conditions, which incorporates hot-gas radiation and the entrainment of the liquid phase into the gas. The approach involves the modelling of the liquid phase as a control volume with constant properties and the evaporation is calculated by means of mass and energy balances. Mass transfer via entrainment is obtained by suitable correlation available in literature [7]. The model includes convection and radiation at the interface of liquid film with combustion gas assuming the liquid phase heating process from the injection temperature to the saturation value as instantaneous. In such a way, an overall vaporization enthalpy can be defined. The evaporation process is modelled similarly to Grisson model [11], i.e., calculating a “dry wall” convective heat transfer coefficient h_0 and then introducing the transpiration correction to obtain h. The radiative heat flux towards the liquid film is calculated using the total hot-gas emittance obtained through the Leckner correlation [21]. Once the evaporation rate is known, the correlation by Sawant et al. [7] is used to calculate the coolant loss due to entrainment, expressed as a fraction E of the injected mass flow rate. Knowing the entrained fraction, the liquid mass flow rate available for film cooling is obtained as $\Gamma_{av} = \Gamma(1 - E)$, and the film cooled length is $FCL = \Gamma_{av}/\dot{m}_{vap}$. Boundary layer model is taken from Grisson model [11]

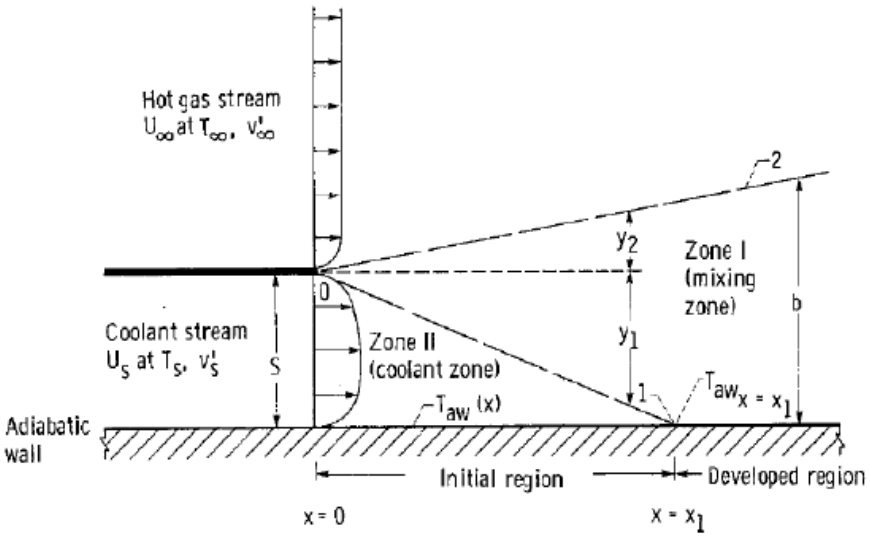

Figure 2. Geometry of the developed flow as assumed by Simon's model [19]

4.4. Di Matteo et al. – Sapienza

Gaseous film cooling model by Di Matteo et al. [20], then modified in the framework of the present activity, is a quasi-2D differential formulation to study the developed flow field of a film wall jet in rocket combustion chambers. It is capable to provide a prediction of the evolution in space and time of both wall heat flux and film cooling effectiveness. The geometry of the developed flow field is based on the one carried out by Simon [19] (see Figure 2. *Geometry of the developed flow as assumed by Simon's model [19]*), which includes three different regions: the core (hot gases), film, and mixing region. The entrained mass flow rates and the quantities exchanged between the hot gas, the mixing, and the film zone are computed by means of geometrical correlations. All the three zones are assumed to have the same pressure for any given cross-section of the combustion chamber, determined as no film cooling were present. The length of the film region (x_1 in Figure 2. *Geometry of the developed flow as assumed by Simon's model [19]*) and the growth rate of the mixing region are calculated first. The former defines the region characterized by coolant properties, so the convective heat flux is determined by film conditions, whilst in the fully developed region the wall conditions are determined by the mixing conditions. An iterative procedure [19] or a CFD-based correlation developed by Sapienza [22] can be used to evaluate x_1. The mixing zone growth rate is calculated as a function of jets densities and velocities.

Flowfield geometry, shown in Figure 2. *Geometry of the developed flow as assumed by Simon's model [19]*, is then computed by knowing $\frac{db}{dx}$ and x_1. The least number of differential equations has been chosen to be included in the model, for simplicity. In particular, all the three governing equations are retained for the core region as in the original ESPSS combustor, whereas the film region is modelled only by means of the energy conservation equation. The latter is written as:

$$V_{film}(\dot{\rho e_0})_{film} = -\Delta(\dot{m}h_0)_{film} - q_{film} \qquad \text{Eq.5}$$

where: V_{film} is the film region volume, $(\rho e_0)_{film}$ is the product between film density and total energy, $(\dot{m}h_0)_{film}$ is the film total enthalpy flux, and q_{film} is the heat flux exchanged by the film region. Quantity (ρe_0) is intended as a single variable being density not provided by mass conservation equation or other procedures. Mass flow rate is supposed to be constant in space but variable in time, and equal to the value at the coolant injector. This occurs as if mass flow rate information propagates with infinite speed for a fixed time instant. Knowing mass flow rate and thus mass flux $G = (\dot{m}/A)_{film}$ also from the geometry, the film thermodynamic state is calculated iteratively. The mixing region properties are determined by those of the hot gas and the coolant in a one-way dependency. Algebraic equations based on geometrical considerations and on the fluid properties of the hot gas and coolant are used to evaluate the incoming energy fluxes to the mixing region. Temperature in mixing volumes is calculated by averaging all the incoming flow temperatures, using their mass flow rate as weights. Since pressure is known from the core region, the density in mixing volumes can be obtained by the equation of state. Effects of area

variation and jet velocities difference are considered on mixing zone velocity.

5. TEST CASES

Experimental test cases have been also selected from the literature to validate the models presented above for liquid and gaseous film cooling. An overview of the chosen test cases is provided in the following.

Selected experimental test cases include 2 tests for liquid film cooling [23, 24] and 2 tests for gaseous film cooling [25, 26]:

5.1. Morrell

The investigation [23] consists in a series of 4 tests employing a liquid oxygen/liquid ammonia thrust chamber, using water as coolant. Wall heat load, thrust, and film cooled length are evaluated in an 8.5 inches long test section located downstream of the injection plate. Coolant injection occurs by means of tangential-slot injectors at the beginning of the test section. Investigations have been performed using different propellant and coolant mass flow rates (see Table 1. *Operating conditions used in [23]*). Available observables are the film cooled length, thrust, and the integral heat load. Heat load is computed from temperature measurements performed with thermocouples adding the vaporization heat where the liquid phase is present. No details on the temperature and heat profiles are reported, heat integral value only.

Table 1. Operating conditions used in [23]

Test no.	Oxidizer mfr (kg/s)	Fuel mfr (kg/s)	Film mfr (kg/s)
# 8	0.99	0.70	0.836
# 9	1.05	0.69	0.836
# 10	1.16	0.66	0.093
# 11	1.14	0.68	0.095

5.2. Kim et al.

Test hardware features a film and regeneratively cooled-liquid oxygen/kerosene calorimetric combustion chamber [24]. Operating conditions are shown in Table 2. *Operating conditions used in [24]* Kerosene is used as film coolant and is injected tangentially right at the injector plate, whereas ambient-temperature water is used in the 19 cooling channels circuits. Cooling channels are used during the experiment to provide heat flux measurements, which are performed by evaluating the total enthalpy difference between cooling circuits manifolds. The presence of many cooling circuits ensures a good spatial resolution for measurements. Observables are average hot gas side wall temperature, characteristic velocity, and axial profiles of wall heat flux.

Table 2. Operating conditions used in [24]

Chamber pressure (bar)	O/F	Oxidizer mfr (kg/s)	Fuel mfr (kg/s)	Film mfr (kg/s)
52.5	2.77	4.42	1.59	0.166

5.3. Arnold et al.

The experiment is an investigation of film cooling performances in a high-pressure liquid oxygen/gaseous hydrogen combustion chamber made up by 5 segments [25]. Coolant is gaseous hydrogen, which is injected right at the injection plate by means of 10 rectangular slots. Information about heat load distribution is provided on the hot inner surface of the combustion chamber at real rocket engines conditions and pressures up to 115 bar.
Operating conditions are shown in Table 3. *Operating conditions used in [25]*. Available observables are axial measurements of wall heat flux. Hot gas-side wall temperature is provided so it is possible to use it as boundary condition to retrieve the heat flux numerically.

Table 3. Operating conditions used in [25]

Oxidizer mfr (kg/s)	Fuel mfr (kg/s)	Film mfr (kg/s)
3.6	0.6	0.084 (2% tot)

5.4. Sulsov et al.

Film cooling performances in a low-pressure gaseous oxygen/gaseous methane combustor are investigated [26]. Operating conditions are shown in Table 4. *Operating conditions used in [26]*. Coolant is ambient-temperature methane, which is injected right at the injection plate by means of a ring injection slot. The investigation focuses on the interaction of the reacting flow with film cooling in the cylindrical part of the combustion chamber near the injector plate, eventually providing information on heat loads distribution at chamber pressure up to 12 bar. Hot gas-side wall temperature is provided so it is possible to use it as boundary condition to numerically retrieve the heat flux, whose measurements are available.

Table 4. Operating conditions used in [26]

Oxidizer mfr (kg/s)	Fuel mfr (kg/s)	Film mfr (kg/s)	Film injection slot height (mm)
0.335	0.1	0.087 (20% tot)	0.46

6. RESULTS

6.1. LFC Validation

Starting with LFC, experimental data by Morrell [23] are compared to numerical results in Table 6. *Experimental and estimated observables by Morrell [23] and present LFC models. "Q" stands for integral heat load.*. The mixing process between the coolant and the hot gas provides a good estimation of the thrust which is in good agreement with experimental data for all the three LFC models for each test. In fact, all the three formulations model the chamber pressurization due to coolant injection. Film cooled length tends to be overestimated by all the models, in each test case, even if acceptable ranges of errors are provided (average is of about 15%). As expected, the best evaluations are provided by the most detailed model, i.e., Grisson model in full formulation. As expected, 0-D models (Simplified Grisson and Shine et al) return higher errors with respect to Grisson full formulation due to their higher level of simplification. They show a significantly similar behavior dealing with this specific test case. Between the two, Shine model seems to give a slightly better accuracy in the FCL estimation.

Full Grisson model is the only one that can be considered reliable when comparing integral heat loads, since it employs a specific and detailed modeling for the estimation of the heat exchange coefficients. Moreover, it gives the best estimation of the FCL, which is a key parameter when comparing the integral heat load since the temperatures of the liquid phase and of the evaporated boundary layer might be very different and might influence such an observable a lot.

Observables by Kim et al. [24] are reproduced using the LFC models in Table 5. *Comparison between Kim et al. scalar observables [24] and numerical results* and Fig.3

Table 5. Comparison between Kim et al. scalar observables [24] and numerical results

	EXP	Full Grisson	Simplified Grisson	Shine et al.
Average Tw [K]	610	668,2	576,8	796
Error (%)	-	9,54	-5,44	30,49
Characteristic velocity (m/s)	1670	1730	1728	1702
Error (%)	-	3,59	3,47	1,91

Table 6. Experimental and estimated observables by Morrell [23] and present LFC models. "Q" stands for integral heat load.

	TEST #8				TEST #9			
	EXP	Full Grisson	Simplified Grisson	Shine et al	EXP	Full Grisson	Simplified Grisson	Shine et al
Thrust, kgf	404.6	382.3	381.4	391.7	397.3	384	383.4	383.6
Error, %	-	-5.52	-5.73	-5.65	-	-3.34	-3.49	-3.45
FCL, m	0.1879	0.2167	0.221	0.2193	0.2073	0.2236	0.2343	0.229
Error, %	-	15.32	17.61	16.71	-	7.86	13.03	10.46
Q_tot, BTU/lb	876	829.9	not reliable	not reliable	871	823.2	not reliable	not reliable
Error, %	-	-5.26	-	-	-	-5.49	-	-
Q_conv, BTU/lb	732	706.9	not reliable	not reliable	736	701.74	not reliable	not reliable
Error, %	-	-3.42	-	-	-	-4.65	-	-
Q_rad, BTU/lb	144	123	not reliable	not reliable	135	121.47	not reliable	not reliable
Error, %	-	-14.55	-	-	-	-10	-	-
	TEST #10				TEST #11			
	EXP	Full Grisson	Simplified Grisson	Shine et al	EXP	Full Grisson	Simplified Grisson	Shine et al
Thrust, kgf	415.9	393.88	393.53	394	415.9	397.56	397	397
Error, %	-	-5.29	-5.37	-5.27	-	-4.40	-4.54	-4.54
FCL, m	0.2042	0.2419	0.2671	0.2549	0.2174	0.2411	0.2663	0.2537
Error, %	-	18.46	30.8	24.82	-	10.90	22.49	16.69
Q_tot, BTU/lb	856	559	not reliable	not reliable	856	560	not reliable	not reliable
Error, %	-	-34.69	-	-	-	-34.58	-	-
Q_conv, BTU/lb	731	450	not reliable	not reliable	721	456.02	not reliable	not reliable
Error, %	-	-38.44	-	-	-	-36.75	-	-
Q_rad, BTU/lb	125	110	not reliable	not reliable	135	103.9	not reliable	not reliable
Error, %	-	-12	-	-	-	-23.04	-	-

Performances, in terms of characteristic velocity, are well predicted by each of the three models. Errors are confined below the 4% threshold. This proves that the assumptions made on the mixing process between the evaporated coolant and the hot gases are appropriate.
Also wall temperatures are in good agreement with experimental data. As expected, also here the complete Grisson model shows the best results with an error of 9.5% with respect to the experiment, whereas the highest discrepancy is showed by Shine model which overestimates the wall temperature by a factor of 30.5%.
The lowest error on the average wall temperature prediction is provided by the Simplified Grisson model, which provides a better prediction than the full formulation. Although the temperature averaging process is not explained in detail in the paper, this aspect is quite unexpected because of the low reliability expected by 0-D models concerning heat transfer evaluation. One possible explanation might lie in the interplay of two different errors. On one hand, 0-D models (as Shine et al.) generally tend to overestimate wall temperature. On the other hand, simplified Grisson model provides a higher film cooled length (FCL) than the other two models, as can be observed from the plot above, thus considering a higher wall region with low temperature which contributes to decrease the average value in the combustion chamber. As a possible consequence of this combined and counterbalanced effect, what is observed is an average wall temperature which is close to experimental data. The effect might be case dependent.

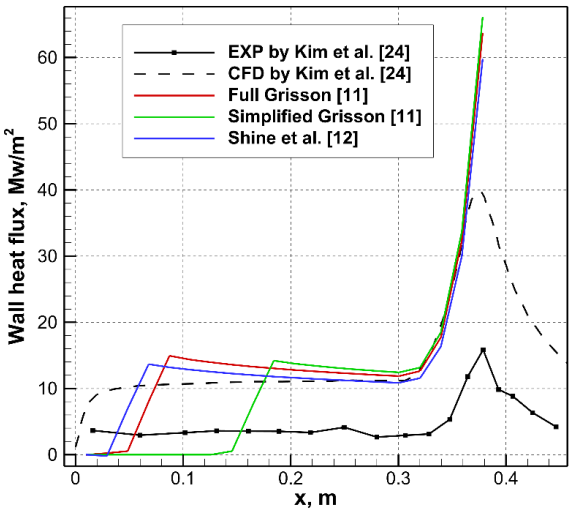

Figure 3. Comparison between experimental [24] and numerical results. CFD by Kim et al. is also included

Concerning convective heat fluxes, all the three liquid film cooling models (red, green, and blue solid lines) provide similar results and overestimate experimental data (black solid line with symbols). However, it must be pointed out that the results are in good agreement with the simulations performed by Kim et al. and reported in the paper. Such fact might be due to some physics happening in the experiment which is not properly modeled numerically.

6.2. GFC Validation

Going further to GFC, Figure 4. *Comparison between experimental data by Arnold et al. [25] and numerical results.* shows the comparison between experimental data by Arnold et al. [25] and numerical results obtained by means of the Di Matteo et al. [20] – Sapienza reduced model, focusing on the chamber region where measurements are available. Numerical solution is in overall good agreement with experimental data, which are also affected by some uncertainty. The maximum punctual error is in the range of 17% and it is obtained in the fully mixed region. Heat flux trend is well predicted. The model is capable of capturing the heat flux ramp in the vicinity of the injection plate due to combustion development and to the film presence in this case.
Even if no measurement point is available in the nozzle, the higher the heat flux values are, the lower the error seems to be. In particular, the last two measurement points values are reproduced within their experimental error bars.
Eventually, the comparison between experimental data by Suslov et al. [25] and numerical results for oxygen/methane propellant combination are shown in Figure 5. *Comparison between experimental data by Suslov et al. [26], reduced model numerical results, and CFD simulation by Betti et al. [27].*. A CFD simulation performed by Betti et al. [27] for the same test case and operating conditions is also shown.

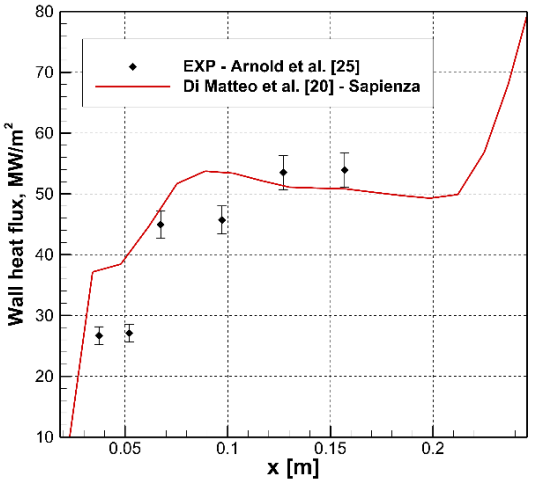

Figure 4. Comparison between experimental data by Arnold et al. [25] and numerical results.

Experimental wall heat flux is well reproduced by the gaseous film cooling model by Di Matteo et al. [20] and Sapienza. The maximum punctual error is in the range of 19% with respect to the experimental data, and it is obtained downstream in the fully mixed region.
The typical initial heat release ramp due to combustion development and to the film presence and mixing is well captured.
A higher film extension is obtained by the numerical model (red line), and thus higher errors are shown close to the injection region.
Errors with respect to experiments appear to be of the same order of magnitude of the ones obtained with the more complex CFD simulation, confirming the reliability of the approach.
A second configuration is used to assess the validity of the GFC reduced model in case of oxygen/methane. Such configuration foresees the same propellant mass flow rates shown in Table 4. *Operating conditions used in [26]*, but using a lower film mass flow rate of 0.022 kg/s (i.e. 5% of the total mass flow rate) and a film injection slot height of 0.2 mm. CFD simulations have been performed to provide a term of comparison for the GFC reduced model results, including also a further case with no film. Results are shown in Figure 6. *Comparison between reduced model results and CFD simulations.*.
Reduced model solution (red line) is in good agreement with that provided by CFD simulation (black line). The maximum punctual error is in the range of 18% with respect to the simulation results. A further solution without film cooling (blue line) is included in the comparison to show the influence of coolant injection on the wall heat flux.
Although some discrepancies are present, wall heat flux trend is well predicted. Particular precision is shown approaching the plateau in the first half of the chamber, where the two solutions (red and black lines) are almost overlapped.

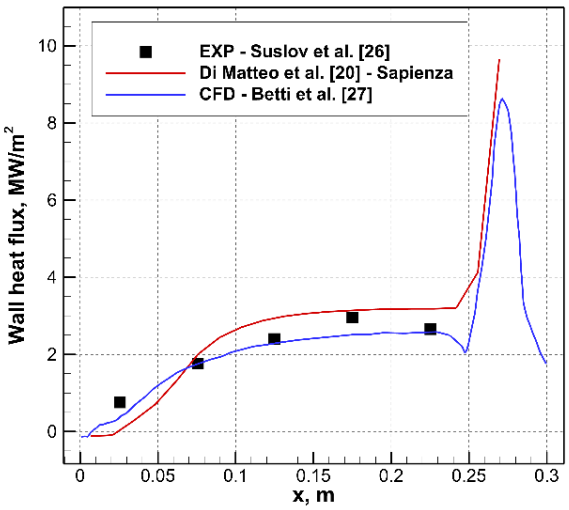

Figure 5. Comparison between experimental data by Suslov et al. [26], reduced model numerical results, and CFD simulation by Betti et al. [27].

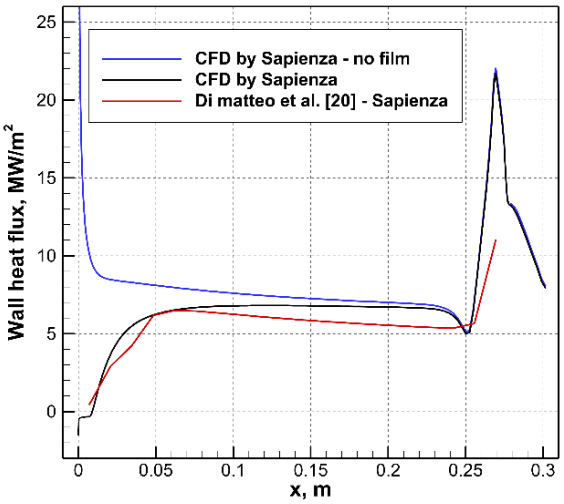

Figure 6. Comparison between reduced model results and CFD simulations.

By looking at both Figures Figure ***5.*** *Comparison between experimental data by Suslov et al. [26], reduced model numerical results, and CFD simulation by Betti et al. [27].* and Figure ***6.*** *Comparison between reduced model results and CFD simulations.*, it can be said that the Di Matteo-Sapienza model is validated against gaseous film cooling test cases, showing an accuracy with respect to experimental data which is comparable to that of more complicated CFD simulations.

7. CONCLUSIONS

An extensive literature review allowed to gather and select the most suitable low-order models of liquid and gaseous film cooling to be implemented in the EcosimPro/ESPSS framework. After a brief presentation of the formulations, this study aimed at assessing and validating the best candidate models in case of liquid rocket engine applications.

Three liquid film cooling models with different level of detail have been validated against the few experimental data found in the literature. All of them have shown low errors around 5% on thrust and characteristic velocity, indicating a correct evaluation of performance losses yielded by cold film injection. Higher but still acceptable errors around 15% have been obtained on film cooled length results, depending in particular on the level of approximation which characterize each formulation. Despite the reasonable agreement between experimental data and numerical results, it can be concluded that liquid film cooling is a challenging phenomenon to be described in detail using low-order models due to the complex underlying phenomena. A comprehensive treatment should take into account all the phenomenology occurring in the combustion chamber, eventually leading to heavy computational burdens, which are not to be sought in the framework of system simulators as ESPSS.

Concerning gaseous film cooling, a single model has been selected, improved and validated against oxygen/hydrogen and oxygen/methane applications. Similar results have been obtained in the two cases, with errors not exceeding 20% on the total wall heat flux along the combustion chamber. Discrepancies are comparable with those obtained by more complex and detailed CFD simulation under different operating conditions, confirming the heat load prediction capability of low-order models in case of gaseous film cooling.

ACKNOWLEDGEMENTS

This research has been supported by European Space Agency (ESA), within the frame of Contract No. 4000129564/19/NL/MG.

REFERENCES

[1] Knuth, E. L. *The mechanics of film cooling*. Diss. California Institute of Technology, 1954.
[2] Crocco, L. "An approximate theory of porous, sweat, or film cooling with reactive fluids." *Journal of the American Rocket Society* 22.6 (1952): 331-338.
[3] Graham, A. R. *Film cooling of rocket motors,* , (Ph.D. thesis), Jet Propulsion Center, Purdue University, 1958.
[4] Sellers, J.P., Experimental and Theoretical Study of the Application of Film-cooling to a Cylindrical Rocket Thrust Chamber, (Ph.D. thesis), Jet Propulsion Center, Purdue University, 1958.
[5] Shembharkar, T. R., and Pai, B. R.. "Prediction of film cooling with a liquid coolant." *International journal of heat and mass transfer* 29.6 (1986): 899-908.
[6] Gater, R. A., L'Ecuyer, M. R. and Warner, C. F.. *Liquid-film cooling, its physical nature and theoretical analysis*. No. JPC-413. Purdue University Lafayette Jet Propulsion Center, 1965.
[7] Sawant, Pravin, Mamoru Ishii, and Michitsugu Mori. "Droplet entrainment correlation in vertical upward co-current annular two-phase flow." *Nuclear Engineering and Design* 238.6 (2008): 1342-1352.
[8] Coy, E.B., Schumaker, S.A. and Lightfoot, M.A.. *Film cooling of liquid hydrocarbon engines for operationally-responsive space access*. No. AFRL-RZ-ED-TP-2010-087. AIR FORCE RESEARCH LAB EDWARDS AFB CA PROPULSION DIRECTORATE, 2010.
[9] Ewen, R.L., and Evensen, H.M.. Liquid rocket engine self-cooled combustion chamber. *NASA space vehicle design criteria (chemical propulsion)*, NASA SP-8124, 1977.
[10] Trotti, M. Modelling of liquid film cooling in aGOX kerosene rocket combustion chamber,Graduate thesis, Politecnico di Milano, 2012.
[11] Grisson, W.M. Liquid film cooling in rocket engines, Technical Report AEDC-TR-91-1, DTIC, 1991.
[12] Shine, S. R., Kumar, S.S., and Suresh B. N. "A new generalised model for liquid film cooling in rocket combustion chambers." *International Journal of Heat and Mass Transfer* 55.19-20 (2012): 5065-5075
[13] Seban, R. A., Chan, H. W., and Scesa, S.. *Heat transfer to a turbulent boundary layer downstream of an injection slot*. American Society of Mechanical Engineers, 1957.
[14] Kacker, S. C., and Whitelaw, J.H. "The effect of slot height and slot-turbulence intensity on the effectiveness of the uniform density, two-dimensional wall jet." J. Heat Transf. 90 (1968): 469-475.
[15] Dellimore, K H., Marshall, A.W., and Cadou, C.P. "Influence of compressibility on film-cooling performance." *Journal of Thermophysics and Heat Transfer* 24.3 (2010): 506-515.
[16] Goldstein, R. J. "Film cooling." *Advances in heat transfer*. Vol. 7. Elsevier, 1971. 321-379.
[17] Goldstein, R. J., and Haji-Sheikh, A.. "Prediction of film cooling effectiveness." *Proceedings of Japanese Society of Mechanical Engineers, Semi-International Symposium*. Vol. 2. 1967.
[18] Arnold, R., Suslov, D., and Haidn, O.J.. "Film cooling of accelerated flow in a subscale combustion chamber." *Journal of propulsion and power* 25.2 (2009): 443-451.
[19] Simon, F. Jet model for slot film cooling with effect of free-stream and coolant turbulence ,NASA

TP2655 (1986).
[20] Di Matteo, F, et al. "Modelling and Simulation of Film Cooling in Liquid Rocket Engine Propulsion Systems." *48th AIAA/ASME/SAE/ASEE Joint Propulsion Conference & Exhibit*. 2012.
[21] Leckner, B., Spectral and total emissivity of water vapor and carbondioxide, Combust. Flame 19 (1972) 33–48.
[22] Sdoga, G. “Tecnica del film cooling in endoreattori a propellente liquido: sviluppo e validazione di un modello empirico mediante simulazioni CFD”, Master thesis, Università di Roma “La Sapienza”, 2020.
[23] Morrell, G. "Investigation of Internal Film Cooling of 1000-pound-thrust Liquid-ammonia-liquid-oxygen Rocket-engine Combustion Chamber." (1951).
[24] Kim, Jong-Gyu, et al. "Film cooling effects on wall heat flux of a liquid propellant combustion chamber." *42nd AIAA/ASME/SAE/ASEE Joint Propulsion Conference & Exhibit*. 2006.
[25] Arnold, R., Suslov, D., and Haidn, O.J.. "Film cooling in a high-pressure subscale combustion chamber." *Journal of propulsion and power* 26.3 (2010): 428-438
[26] Suslov, D, et al. "Experimental Investigation and CFD-Simulation of the Film Cooling in an O2/CH4 subscale Combustion Chamber." *Space Propulsion Conference*. 2012.
[27] Betti, B, et al. "Numerical study of heat transfer in film cooled thrust chambers." *48th AIAA/ASME/SAE/ASEE Joint Propulsion Conference & Exhibit*. 2012.
[28] Vilá J., Moral J., Fernández-Villacé V., Steelant J., ‘An Overview of the ESPSS Libraries: Latest Developments and Future', *Space Propulsion 2018*, Seville, Spain, 14-18 May 2018, SP2018-00572.